MOLECULAR AND CELLULAR BIOLOGY, Dec. 2001, p. 8276–8288 Vol. 21, No. 24
0270-7306/01/$04.00+0 DOI: 10.1128/MCB.21.24.8276–8288.2001

Resistance to Tumor Necrosis Factor-Induced Cell Death Mediated by PMCA4 Deficiency†

KOH ONO, XIAOFEI WANG,‡ AND JIAHUAI HAN*

Department of Immunology, The Scripps Research Institute, La Jolla, California 92037

Received 28 June 2001/Returned for modification 20 August 2001/Accepted 12 September 2001

We used retrovirus insertion-mediated random mutagenesis to generate tumor necrosis factor (TNF)-resistant lines from L929 cells. Using this approach, we discovered that the plasma membrane calcium ATPase 4 (PMCA4) is required for TNF-induced cell death in L929 cells. Under basal conditions, PMCA4-deficient ($PMCA^{mut}$) cells have a normal phenotype. However, stimulation with TNF induces an abnormal increase in the intracellular calcium concentration ($[Ca^{2+}]_i$). The substantially elevated $[Ca^{2+}]_i$ caused resistance to TNF-induced cell death. We found that an increase in the total volume of acidic compartments (VAC), mainly constituted by lysosomes, is a common event in cell death caused by a variety of agonists. The increased $[Ca^{2+}]_i$ in $PMCA^{mut}$ cells promoted lysosome exocytosis, which, at least in part, accounted for the inhibition of TNF-induced increase in VAC and cell death. Promoting lysosome exocytosis by calcium inhibited TNF-induced cell death in wild-type L929 cells, while inhibition of lysosome exocytosis or increase of VAC by sucrose restored the sensitivity of $PMCA^{mut}$ cells to TNF-induced cell death. Thus, increase of the volume of acidic compartment is a part of the cell death process, and the antideath effect of calcium is mediated, at least in part, by inhibition of the TNF-induced increase in VAC.

The involvement of calcium in cell death has been widely reviewed over the last several decades. A prevalent assumption is that either a low or high intracellular calcium concentration ($[Ca^{2+}]_i$) can cause cell death because of the critical role played by calcium in many physiological processes. However, it has also been shown that calcium can promote cell survival in a number of systems. For example, a modest elevation of $[Ca^{2+}]_i$ above normal resting levels (100 to 150 nM) can promote cell survival in developing neurons (20).

The proapoptotic effects of calcium can vary across cell types and may be mediated by different mechanisms. For example, calcium-dependent induction of Nur77 gene expression is essential for T-cell receptor-induced death in thymocytes (92), whereas calcium-induced activation of calcineurin has been implicated in calcium-induced cell death in other cell types (88). The mechanisms underlying these two types of cell death are relatively clear. Both Nur77 and calcineurin trigger mitochondrial release of cytochrome *c* and subsequent cell death. The former occurs via direct translocation onto mitochondria (47), and the latter occurs via dephosphorylation of Bad to initiate mitochondrial response (88).

On the other hand, very little is known about calcium-mediated resistance to cell death. Calcineurin has also been suggested to be involved in calcium-mediated cell protection (52). Furthermore, p38 mitogen-activated protein kinase-dependent activation of MEF2C activation may be involved in the calcium-dependent survival of neurons (53, 63). The mechanism by which calcium prevents cell death under these conditions is unknown.

It has been well accepted that the principal role of the lysosome is one of cellular housekeeping. Lysosomes remove damaged macromolecules from the cellular environment and convert them into reusable products. However, recent works demonstrated that lysosomal exocytosis occurs in many cell types, suggesting that this organelle may not be just a final station of the endocytic pathway but may have other functions (2, 25, 75, 76, 85). At one time, lysosomes were proposed to be "suicide bags," or prepackaged destruction awaiting a programmed instruction to strike (14). The suicide bag theory has not endured because it lacks supporting evidence (50). However, the possibility that lysosomes play a role in cell death cannot be excluded, since over the past 40 years, many groups of investigators have observed alterations in lysosomes during cell death (14, 51, 60).

Leakage of lysosomes has been observed morphologically in several models of cell death, including death caused by oxidative stress and by serum deprivation (7, 65). Autophagy was associated with death in several different cell types, and inhibition of autophagy prevented apoptosis induced by withdrawal of nerve growth factor (36, 62, 91). The role of the lysosome in cell death was further supported by the observation that various lysosomotropic agents, such as ammonium chloride and chloroquine, can prevent certain types of cell death, such as that induced by tumor necrosis factor alpha (TNF) (43, 49, 58). The lysosomal protease cathepsin D is involved in a number of types of apoptosis, including that induced by gamma interferon, Fas, and TNF (15, 28, 34, 67, 73). Although the available data are somewhat limited, there is a growing body of evidence suggesting that lysosomes actively participate in cell death.

TNF is a proinflammatory cytokine that acts as a mediator of host defense as well as inflammatory diseases (3, 4). TNF was

* Corresponding author. Mailing address: Department of Immunology IMM-32, The Scripps Research Institute, 10550 North Torrey Pines Road, La Jolla, CA 92037. Phone: (858) 784-8704. Fax: (858) 784-8665. E-mail: jhan@scripps.edu.

† This is publication no. 14231-IMM from the Department of Immunology, The Scripps Research Institute, La Jolla, Calif.

‡ Present address: Avigen, Inc., Alameda, CA 94502.

originally identified and purified as a factor that leads to rapid hemorrhagic necrosis of an established tumor (9, 64). It is now known that TNF can induce cell death in numerous cell types, and it is widely used to study the mechanisms of cell death. The morphological characteristics of cells differ markedly among various TNF-treated cell lines. For example, TNF induces an apoptotic phenotype (chromatin condensation and cell shrinkage in a nearly or wholly intact plasma membrane) in MCF-7, KYM, and PC60 tumor cell lines (19), whereas L929 and WEHI 164 clone 13 cells respond to TNF with characteristics of necrosis (5, 19).

It is known that death signaling in both apoptotic and necrotic cell death is initiated by clustering of the TNF receptor-1 and recruitment of the death domain-containing adapter protein TRADD (1, 19, 33). The subsequent apoptosis of TNF-treated cells is mediated by activation of caspases and release of cytochrome *c* from the mitochondria (48, 82, 83), while the necrotic cell death of L929 cells is independent of caspases (86).

In an effort to identify genes that mediate the cytolytic effect of TNF, we have used a random gene disruption approach to generate a series of L929 mutants that are resistant to TNF-induced cell death. The gene disrupted in one of the TNF-resistant lines was identified as PMCA4, a ubiquitously expressed protein that couples the extrusion of calcium across the plasma membrane with ATP hydrolysis (22, 27). To date, four PMCAs (PMCA1 to -4) have been identified. PMCA1 and PMCA4 are expressed in almost all tissues, whereas PMCA2 is expressed primarily in brain and heart and PMCA3 expression is essentially confined to brain and skeletal muscle. PMCAs were believed to be Ca^{2+} pumps that maintain basal levels of intracellular calcium (22, 27). Here we show that resistance to cell death in PMCA4-deficient L929 fibroblasts is mediated by a modest elevation in $[Ca^{2+}]_i$. We found that an increase in lysosome volume is a common feature of cells that undergo either apoptotic or necrotic cell death. We further show that increased levels of $[Ca^{2+}]_i$ in PMCA4-deficient cells enhanced lysosomal exocytosis. This increase in $[Ca^{2+}]_i$ levels accounts, at least in part, for the diminished lysosomal response in PMCA4-deficient cells. The impaired lysosomal response leads, in turn, to TNF resistance.

MATERIALS AND METHODS

Cell culture. All cell lines were obtained from the American Type Culture Collection (Rockville, Md.) and cultured under the recommended conditions. TNF sensitivity was examined in L929 murine fibrosarcoma cells, which exhibited a spontaneous survival rate of less than 1 in 10^6 after 48 h of exposure to TNF at 100 ng/ml. Stable TNF-resistant cell lines derived from L929 cells were established either by retroviral infection or by plasmid transfection with the GenePorter transfection reagent (GTS Inc., San Diego, Calif.). Stably transfected TNF-resistant clones were selected in normal growth medium with the addition of either G-418 (1 mg/ml) or blasticidin S (10 μg/ml) (Invitrogen, Carlsbad, Calif.).

Retroviral vector construction and subcloning. The pDisrup retroviral vector was constructed based on the Moloney murine leukemia virus retroviral vector pLNCX backbone (56). This vector encodes a *neo* gene that is driven by the cytomegalovirus (CMV) promoter, but lacks a poly(A) addition signal sequence (89). Standard recombinant DNA techniques were used in vector construction and subcloning. The splicing donor and acceptor sites were designed based on the human adenovirus type 2 major late mRNA intron sequence. Incorporation of the splicing donor sequence downstream from the *neo* coding sequence permitted the generation of a *neo* mRNA fused with the downstream exon of a disrupted gene if viral insertion occurred within an intron. If the virus inserted within an exon, the expressed *neo* mRNA should represent a direct fusion with endogenous exon sequences at the insertion site. *neo* mRNA cannot be expressed if the insertion occurs in a nongene region. Further details of the retroviral plasmid are available upon request. The PMCA4 cDNA was obtained from Ernst Carafoli and subcloned into the pcDNA6 expression vector, which carries blasticidin resistance (Invitrogen, Carlsbad, Calif.).

Retrovirus production and cell infection. pDisrup recombinant retroviruses were generated in Phoenix Amphotropic producer cells using the calcium phosphate method of transfection (56). Viruses were produced at 32°C, and virus-containing medium was collected 24 h posttransfection and filtered through a 0.45-μm filter. L929 cells were plated in six-well plates at a density of 5×10^5 cells/well. One round of retroviral infection was performed by replacing medium with 2 ml of pDisrup virus (containing 4 μg of Polybrene per ml), followed by centrifugation of the six-well plates at 2,500 rpm for 30 min at 32°C.

3′-RACE. The portion of the endogenous gene that was fused with the *neo* gene was amplified by the 3′ rapid amplification of cDNA ends (RACE) technique. Total RNA was isolated, and reverse transcription was performed with the primer 5′-CCA GTG AGC AGA GTG ACG AGG ACT CGA GCT CAA $GC[T]_{17}$-3′. A nested PCR was performed with the resulting reverse transcription product with the following primers: P1/Q1 (5′-ATG GGC TGA CCG CTT CCT-3′ and 5′-CCA GTG AGC AGA GTG ACG-3′) and P2/Q2 (5′-GAC GAG TTC TTC TGA CTA GCT AG-3′ and 5′-GAG GAC TCG AGC TCA AGC-3′). P1 and P2 are located on the *neo* resistance gene, while Q1 and Q2 are on the anchor sequence of QT. The PCR fragments were subcloned into the TA cloning vector (Invitrogen) and subjected to DNA sequencing.

Western blot analysis. Crude membranes were prepared as described (27) and subjected to sodium dodecyl sulfate–6% polyacrylamide gel electrophoresis, followed by standard Western blotting procedures. The monoclonal antibody 5F10 (Affinity Bioreagents, Inc, Golden, Colo.) was used to detect total PMCA immunoreactivity.

Measurement of intracellular calcium. Cells were loaded with 4 μg of fluo-3 acetoxymethyl (AM) (Molecular Probes, Inc., Eugene, Oreg.) and 10 μg of Fura-Red AM (Molecular Probes, Inc.) per ml in the presence of 4 mM probenecid (Sigma, St. Louis, Mo.) at 37°C for 1 h, according to published protocols (61). Flow cytometry analysis was performed at 488 nm excitation, the fluorescence of fluo-3 was collected at 520 nm, and Fura-Red emission was collected at 640 nm. An in situ calibration assay for calcium measurements in L929 cells was performed as described (37). The fluo-3/Fura-Red ratio versus calcium concentration was plotted and used to calculate $[Ca^{2+}]_i$ in each sample as described (37).

Measurement of VAC. Cells in various stages were harvested and then incubated at 37°C for 15 min with 100 ng/ml LysoTracker (Molecular Probes, Inc.) or 5 μg/ml acridine orange (AO) (Sigma, St. Louis, Mo.). Cells were then washed, pelleted, and resuspended in 1 ml of phosphate-buffered saline (PBS) for measurement of fluorescence derived from the aggregated LysoTracker or AO in acidic compartments. The healthy cells (with intact lysosomes) were gated, and the mean value of the fluorescence intensity was used as the relative value of total volume of the acidic compartment (VAC).

Cell viability assay using PI staining plus forward-angle light scattering. The integrity of the plasma membrane was assessed by the ability of cells to exclude propidium iodide (PI) (Sigma, St. Louis, Mo.). Cells were trypsinized, collected by centrifugation, washed once with PBS, and resuspended in PBS containing 1 μg/ml PI. The levels of PI incorporation were quantified by flow cytometry on a FACScan flow cytometer. Cell size was evaluated by forward-angle light scatting. PI-negative cells of normal size were considered live cells.

Measurement of lysosme pH. Double fluorescein- and tetramethylrhodamine-labeled dextran (FTD) (Molecular Probes) was used as a ratiometric indicator to study the pH change of lysosomes. L929 cells were labeled with FTD (3 mg/ml) for 30 min and then changed to FTD-free medium for 60 min. FTD was internalized and selectively localized in lysosomes (21). The ratio of fluorescein emission at 520 nm to rhodamine emission at 580 nm was used to calculate pH. The calibration and calculation of fluorescein emission-to-rhodamine emission ratio were performed as described (23).

Measurement of intracellular pH. 2′,7′-bis-(2-carboxyethyl)-5-(and -6)-carboxyfluorescein (BCECF) was used as a ratiometric dye for intracellular pH measurement. Cells were loaded with 2 μg of BCECF AM per ml. Emission fluorescences at 525 and 640 nm were collected. The calibration and calculation of the 525 nm:640 nm emission ratio were performed as previously described (11).

Measurement of endocytosis and exocytosis. The endocytosis of TNF-treated L929 cells was measured as described (57, 87). Briefly, the cells were treated with TNF for 0.5, 1, 2, 4, 6, or 8 h and then cultured with dextran conjugated with tetramethylrhodamine (Molecular Probes) (3 mg/ml). The cells were washed

after 30 min, and the uptake of dextran was determined by fluorescence-activated cell sorting (FACS) analysis. Exocytosis was measured by monitoring the release of dextran that was taken up into lysosomes (21). Briefly, cells were labeled with dextran conjugated with tetramethylrhodamine for 30 min. The cells were washed and incubated in dextran-free medium for an additional hour to allow all conjugated dextran to be taken up into lysosomes. The cells were treated with TNF for different periods of time, and the dextran that was retained inside the cells was determined by FACS analysis (21).

β-Hexosaminidase activity assay. Confluent monolayers of L929 cells in culture dishes were washed with PBS and incubated with 0.5 ml of Dulbecco's modified Eagle's medium in the absence of phenol red for the indicated times. *N*-Acetyl-β-D-glucosaminidase (β-hexosaminidase) activity in the culture medium and in the cells was measured as described previously (69).

Transmission electron microscopy. A standard protocol was used to prepare the samples for electron microscopy (45). The experiments were performed by the Core Electron Microscope Facility of the Scripps Research Institute using a Philips CM-100 electron microscope. Specific images were recorded photographically using Kodak SO-163 film.

Electrophoretic mobility shift assay. For the electrophoretic mobility shift assay, nuclear extracts of cells were incubated with a double-stranded, ^{32}P-labeled oligonucleotide containing an NF-κB binding site as a probe as described elsewhere (41)

RESULTS

Disruption of PMCA4 gene in L929 cells confers resistance to TNF-induced cell death. We used retrovirus insertion-mediated mutagenesis in L929 fibroblasts coupled with TNF treatment to select TNF-resistant cell lines that were generated by the mutagenesis. As described in Materials and Methods, the retroviral vector was designed so that the *neo* gene was fused to the sequence of the exon that was at the 3′ end of the viral insertion site. The identities of the disrupted genes in various TNF-resistant cell lines were determined by 3′-RACE of the fused *neo* mRNA.

The gene disrupted in one of the TNF-resistant cell lines was identified as PMCA4. A partial sequence of the fused gene product generated by retroviral insertion in this line (termed PMCA^{mut}) is shown in Fig. 1A. The *neo* gene encoded by the viral vector was inserted at the 5′ end of the PMCA4 coding region and therefore disrupted a PMCA4 gene. Western blotting analysis using a monoclonal antibody that recognizes all PMCA isoforms showed that there was an overall reduction in PMCA immunoreactivity in the PMCA^{mut} cell line compared to parental L929 cells (Fig. 1B). This is consistent with the prediction that the PMCA4 protein level was reduced in PMCA^{mut} cells.

Northern blot analysis using a *neo* probe indicated that there is a single viral insertion in the PMCA^{mut} line (Fig. 1C). The size of the *neo*-PMCA4 fusion mRNA was consistent with the predicted length. To evaluate whether the TNF resistance of the PMCA^{mut} line was due to the lack of PMCA4 expression in these cells, we stably expressed a cDNA encoding PMCA4 under the control of a CMV promoter or empty vector in the PMCA^{mut} cell line (designated reconstituted and vector, respectively). As shown in Fig. 1D, the parental cells and the PCMA4-reconstituted cells (expressing wild-type PMCA4) were highly sensitive to TNF-induced cell death. In contrast, the PMCA^{mut} and vector-transfected cell lines were significantly more resistant to TNF-induced cytotoxity than to the parental and reconstituted cell lines. Thus, the resistance to TNF-induced cell death observed in the PMCA^{mut} cell line is due to the reduced levels of PMCA4 expression in these cells.

Impaired dynamic Ca^{2+} regulation in response to TNF in PMCA^{mut} cells. Since PMCA4 functions in maintaining the basal $[Ca^{2+}]_i$, we next compared $[Ca^{2+}]_i$ in these various cell lines. Calcium concentration was measured by flow cytometry using fluo-3/Fura-Red ratios as described (61). Fluo-3 emits fluorescence upon binding to Ca^{2+} and the fluorescence of simultaneously loaded Fura-Red was used to normalize dye loading. Under basal conditions in normal growth medium, $[Ca^{2+}]_i$ levels were identical in parental L929 cells, PMCA^{mut} cells, PMCA4-reconstituted cells, and vector-transfected cells (Fig. 1E). In contrast, when the cells were treated with TNF, $[Ca^{2+}]_i$ increased by ≈35 nM in parental and in PMCA4-reconstituted cells, whereas $[Ca^{2+}]_i$ increased by ≈100 nM in PMCA^{mut} cells and vector-transfected cells. The higher $[Ca^{2+}]_i$ in PMCA4-deficient cells (Fig. 1E) was correlated with a higher survival rate of these cells after TNF treatment (Fig. 1D), suggesting that the elevation in $[Ca^{2+}]_i$ prevents TNF-induced cell death.

Increased $[Ca^{2+}]_i$ protects against cell death in L929 cells. It has been well established that modest elevations in $[Ca^{2+}]_i$ can prevent cell death in developing neurons (20). The protective effect of increased $[Ca^{2+}]_i$ has also been observed in other systems (52, 70). The data presented in Fig. 1D and 1E suggested that the elevated $[Ca^{2+}]_i$ also protects L929 cells against TNF-induced death. To further establish whether the TNF resistance observed in the PMCA^{mut} line resulted from increases in $[Ca^{2+}]_i$, we treated parental L929 cells with TNF in the presence of various concentrations of either $LaCl_3$, an inhibitor of PMCA (31), or A23187, a calcium ionophore. Both $LaCl_3$ and A23187 treatment elevated $[Ca^{2+}]_i$ and enhanced survival in TNF-treated L929 cells (Fig. 2A and 2B). Optimal protection against TNF-induced cell death was observed at a $[Ca^{2+}]_i$ of ≈200 nM (≈100 nM above the basal level) (Fig. 2A and 2B). Similar $[Ca^{2+}]_i$ levels were observed in PMCA^{mut} cells treated with TNF (Fig. 1E).

L929 cells appear to be insensitive to calcium-induced death, as incubation with the calcium ionophore A23187 did not lead to any detectable cell death (data not shown). Thus, L929 cells may be a good system for the study of the protective role of calcium. To examine whether elevated $[Ca^{2+}]_i$ causes a general resistance to death in L929 cells, we treated parental and PMCA^{mut} cells with various stimuli to trigger cell death, including staurosporine, etoposide, and lonidamine. PMCA^{mut} cells were significantly more resistant to cell death induced by each of these death stimuli than parental L929 cells (Fig. 2C). Cotreatment with A23187 also increased survival of parental L929 cells (Fig. 2C). This suggests that an elevation in $[Ca^{2+}]_i$ has a general role in protecting this cell type from death.

TNF stimulation leads to activation of multiple signaling pathways, including NF-κB (84). To examine whether the deficiency of PMCA4 in L929 cells had a general effect on TNF-induced cellular responses, we compared NF-κB activation in TNF-treated parental and PMCA^{mut} cells by electrophoretic mobility shift assay. As shown in Fig. 3A, there was no detectable difference between parental and PMCA^{mut} cells in NF-κB activation.

To determine whether or not PMCA4 deficiency-mediated TNF resistance requires new protein synthesis, we compared TNF-induced cell death in the presence and absence of a translation inhibitor, cycloheximide. As expected, cyclohexi-

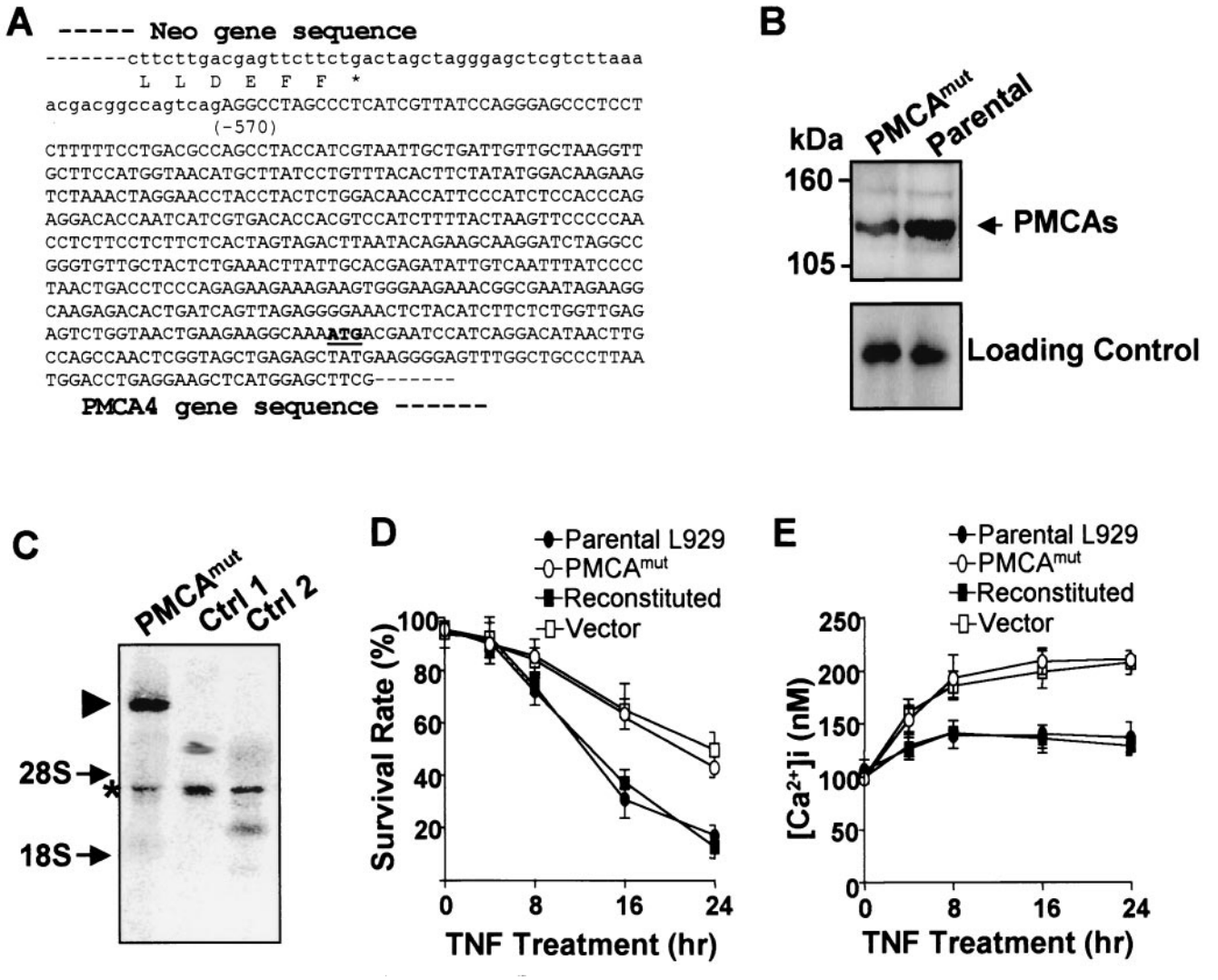

FIG. 1. PMCA4 is involved in TNF-induced cell death, and $[Ca^{2+}]_i$ influences TNF sensitivity in L929 cells. (A) The fused mRNA of *neo* and an endogenous gene in a TNF-resistant L929 clonal cell line was amplified by 3′-RACE. The junction sequence of the fused cDNA is shown, which reveals that the viral insertion occurred at the 5′ end of the PMCA4 gene. Amino acid sequence at the C terminus of *neo* is shown beneath the mRNA sequence. The sequence introduced by viral vector is shown in lowercase. The number in parentheses shows the beginning of the PMCA4 gene relative to its start codon (+1). (B) PMCA protein is reduced in PMCA4 mutant cells ($PMCA^{mut}$). An antibody that recognizes all four PMCA isoforms was used in Western blotting analysis on membrane protein samples from $PMCA^{mut}$ and parental wild-type L929 cells (PMCA1 to -4 are each ≈130 kDa, as indicated by the arrow). A nonspecific band in the Western blot that shown in the lower panel indicates equal protein loading. (C) Total RNA was prepared from $PMCA^{mut}$ and two other clonal cell lines that had viral insertions in other loci. *neo* mRNA levels were analyzed by Northern blot using a ^{32}P-labeled double-stranded *neo* probe. A single *neo* fusion mRNA was detected in $PMCA^{mut}$ cells, as indicated by the triangle. The asterisk indicates transcripts driven by the 5′ long terminal repeat, which was detected in all three lines by the *neo* probe because it contains antisense sequence of *neo*. Arrows show the positions of 28S and 18S rRNA. (D) Stable cell lines were generated from $PMCA^{mut}$ cells by transfection with either a wild-type PMCA4 expression vector (reconstituted) or the empty vector (vector). All three cell lines, together with parental wild-type L929 cells, were treated with TNF (100 ng/ml), and cell viability was determined by PI exclusion plus cell size at various time points (see Materials and Methods for details). The samples were analyzed by flow cytometry (FACScan flow cytometer [Becton Dickinson]) with CellQuest acquisition and analysis software. (E) Parental L929, $PMCA^{mut}$, reconstituted, and vector cells were treated with TNF for various periods of time as indicated. Live cells were gated as in panel D, and $[Ca^{2+}]_i$ was measured by fluo-3 and Fura-Red fluorescence ratios. Data are expressed as average ± standard error of the mean as determined in triplicate samples.

mide enhanced cell death by TNF in both parental and $PMCA^{mut}$ cells (Fig. 3B). A higher survival rate was seen in $PMCA^{mut}$ cells regardless of the presence or absence of cycloheximide, suggesting that PMCA4 deficiency-mediated death resistance is independent of new protein synthesis.

Disruption of calcium regulation may affect lysosomal function in TNF-treated cells. The effect of the PMCA inhibitor $LaCl_3$ and the calcium ionophore A23187 on TNF-induced cell death was compared in cells expressing normal levels of PMCA4 (parental and reconstituted cells) and cells deficient in PMCA4 ($PMCA^{mut}$ and vector-transfected $PMCA^{mut}$) (Fig. 4A). When the samples were treated with TNF alone, parental and reconstituted cells had an average survival rate of less than 20%, while $PMCA^{mut}$ and vector-transfected $PMCA^{mut}$ cells

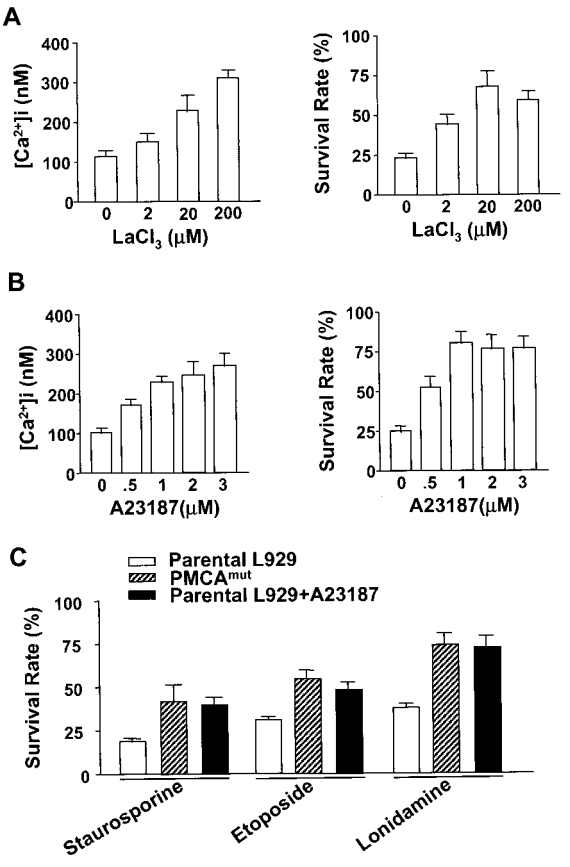

FIG. 2. Increase in $[Ca^{2+}]_i$ induces resistance to cell death in L929 cells. (A) Parental L929 cells were treated with TNF in the presence or absence of various concentrations of $LaCl_3$, an inhibitor of PMCAs, for 24 h as indicated. $[Ca^{2+}]_i$ and cell viability were determined. (B) Parental L929 cells were treated with TNF in the presence or absence of various concentrations of the calcium ionophore A23187 for 24 h as indicated. $[Ca^{2+}]_i$ and cell viability were determined. (C) Parental and $PMCA^{mut}$ cells were treated with staurosporine, etoposide, or lonidamine in the presence or absence of A23187 for 36 h. Cell viability was determined.

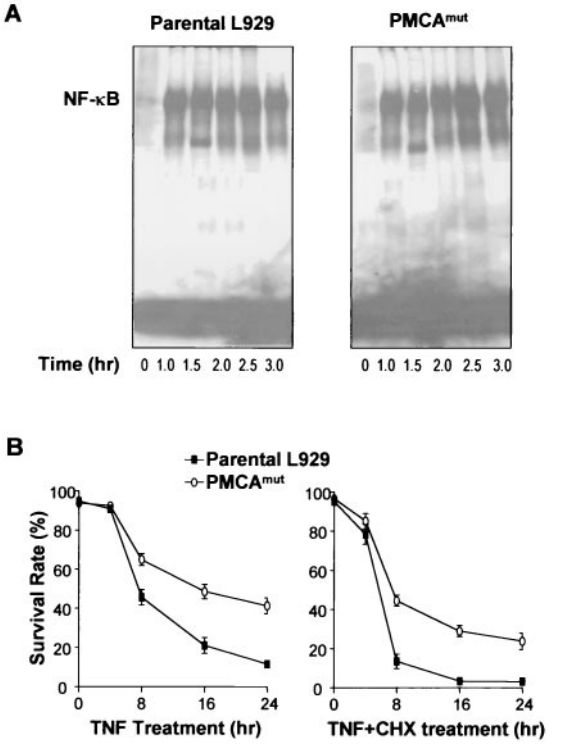

FIG. 3. PMCA4 deficiency did not influence TNF-induced NF-κB activation, and its effect on cell death did not require new protein synthesis. (A) Parental and $PMCA^{mut}$ cells were treated with TNF for different periods of time as indicated. NF-κB activation was measured by electrophoretic mobility shift assay. (B) Parental and $PMCA^{mut}$ cells were treated with TNF or TNF and cycloheximide (CHX, 10 μg/ml) for different periods of time. Cell viability was determined.

had a survival rate of ≈45% (Fig. 4A). There is a more than twofold difference in survival rate between PMCA4-normal and PMCA-deficient cells. However, when the cells were cotreated with $LaCl_3$ or A23187 and TNF, the survival rates of PMCA4-normal and -deficient lines became comparable and increased to ≈50% (Fig. 4A). The similar survival rate of the TNF-treated cells of the four lines in the presence of $LaCl_3$ or A23187 further supported the conclusion that PMCA4 deficiency and $LaCl_3$ and A23187 affected the same event, $[Ca^{2+}]_i$.

We reasoned that blocking other events in this pathway should also lead to equal survival rates between TNF-treated PMCA4-normal and -deficient cells. Therefore, we checked the effect of several other compounds known to inhibit TNF-induced cell death on survival rates in TNF-treated parental, $PMCA^{mut}$, reconstituted, and vector-transfected cell lines. The four cell lines were treated with TNF in the presence or absence of either thenoyltrifluoroacetone (an inhibitor of complex II in the respiratory chain that blocks reactive oxygen species [ROS] formation) or butylated hydroxyanisole (a free-radical scavenger) (Fig. 4B).

Although thenoyltrifluoroacetone and butylated hydroxyanisole enhanced the survival rate of all four cell lines, a markedly higher survival rate persisted in the $PMCA^{mut}$ and vector-transfected cell lines. Similarly, inhibition of phospholipase A_2 by aristolochic acid or inhibition of phospholipase C by D-609 both enhanced the cell survival rate in response to TNF in each of the four cell lines (Fig. 4C). However, a markedly higher survival rate persisted in the $PMCA^{mut}$ and vector-transfected cell lines compared to the parental and reconstituted cell lines. These data suggest that ROS generation and activation of phospholipases A_2 and C are separate pathways from that involving calcium in TNF-treated L929 cells. In contrast, when PMCA4-normal and -deficient cells were cotreated with TNF in the presence of either chloroquine or the protease inhibitor pepstatin A, the survival rates of these cells were increased to approximately the same level (Fig. 4D).

Chloroquine and pepstatin A are known to have many different effects on cells. However, one common effect of chloroquine and pepstatin A is interference with the function of lysosomes. Chloroquine neutralizes lysosomal pH, and pepstatin A inhibits lysosomal proteases (15, 43). We further evaluated the effect of inhibition of lysosome proteases on TNF-induced cell death by using zFA.fmk and N-acetyl-Leu-Leu-Nle-CHO and obtained similar results (data not shown). Thus, it is possible that $[Ca^{2+}]_i$ is intrinsically linked to lysosomal function and that the TNF resistance induced by disruption of the PMCA4 gene is related to lysosomal function.

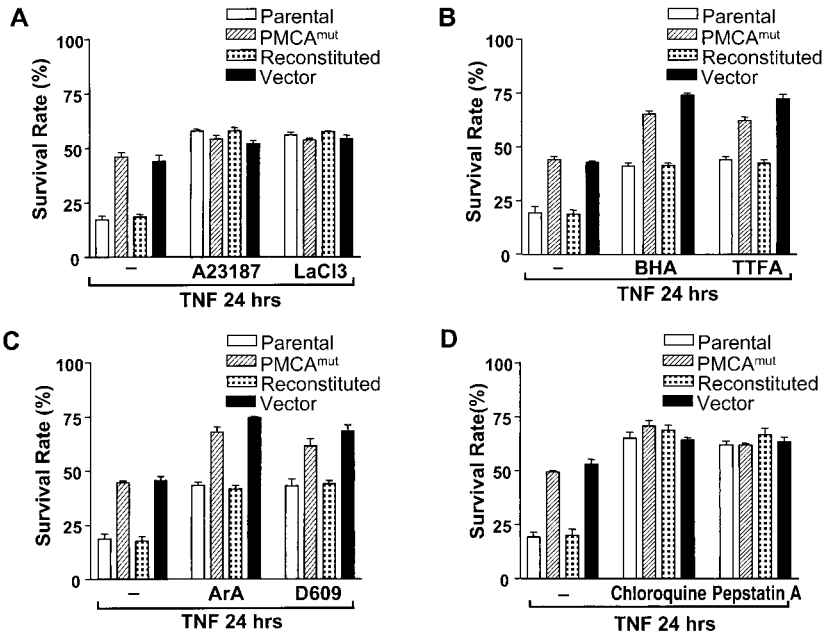

FIG. 4. Increases in $[Ca^{2+}]_i$ and inhibition of lysosomal activity can abolish the differences in TNF sensitivity between parental and PMCA^{mut} cells. Parental L929, PMCA^{mut}, reconstituted, and vector cells were treated with TNF in the presence or absence of various inhibitors, as indicated, and cell viability was determined 24 h later. (A) The four cell lines were cotreated with TNF and either the calcium ionophore A23187 (1 μM) or the PMCA inhibitor $LaCl_3$ (20 μM), and the resulting survival rates are shown. (B) The four cell lines were cotreated with TNF and either the free-radical scavenger butylated hydroxyanisole (BHA, 50 μM) or complex II inhibitor thenoyltrifluoroacetone (TTFA, 250 μM), and the resulting survival rates are shown. (C) The four cell lines were cotreated with TNF and either a phospholipase A_2 inhibitor, aristolochic acid (ArA, 50 μM), or a phospholipase C inhibitor (D-609, 50 μg/ml), and the resulting survival rates are shown. (D) The four cell lines were cotreated with TNF and either chloroquine (25 μM) or pepstatin A (50 μM), and the resulting survival rates are shown.

TNF increases lysosome volume, and disruption of PMCA4 gene impairs this effect. We next asked whether lysosomes are involved in TNF resistance that is associated with disruption of the PMCA4 gene in L929 cells. LysoTracker is an acidotropic probe that can be used to stain lysosomes and other types of acidic compartments. AO is a weak basic amine that selectively accumulates in cellular compartments of low internal pH and is also widely used for staining lysosomes (44, 65). Parental L929 and PMCA^{mut} cells were treated with TNF, stained with LysoTracker and AO, and analyzed microscopically.

As shown in Fig. 5A, TNF treatment significantly increased the accumulation of LysoTracker and AO staining in parental L929 cells, but not in PMCA^{mut} cells. This suggests that the TNF resistance observed in PMCA^{mut} cells is related to the lysosomal response. However, we also considered the possibility that the intensity of LysoTracker and AO staining could be affected by a decrease in lysosomal pH. We used dextran-fluorescein staining and flow cytometry to determine lysosomal pH as previously described (21). These experiments showed that the pH of lysosomes was not lowered but rather slightly increased in response to TNF treatment, thereby excluding the possibility that the increase in LysoTracker and AO staining was due to reduced lysosomal pH (data not shown). LysoTracker and AO staining can also be influenced by the number of late endosomes present in the cell because of the relatively low internal pH in these structures. However, TNF treatment for 0.5, 1, 2, 4, 6, or 8 h had no influence on the rate of endocytosis in L929 cells as measured by dextran uptake (data not shown). Thus, the differences in LysoTracker and AO staining after TNF stimulation in PMCA^{mut} versus parental cells is most likely due to a difference in either the number or the size of lysosomes in these cells.

To determine whether there is an alteration in lysosomes in response to TNF treatment, we analyzed lysosomes in parental and PMCA^{mut} cells by electron microscopy. Electron microscopy confirmed that TNF induced a significant change in lysosomes in L929 but not in PMCA^{mut} cells (Fig. 5B). The electron microscopy pictures shown in Fig. 5B suggested that the increases in lysosome number and size both contributed to the increase in LysoTracker and AO staining in response to TNF stimulation (Fig. 5A).

We monitored lysosomal changes in single cells during the course of TNF-induced L929 cell death. As shown in Fig. 5C, lysosome staining was increased and reached a maximum at 8 h after TNF treatment. The lysosome staining was released at 9 h, and the cells subsequently lost attachment and died, suggesting that lysosome leakage occurred in the later stage of L929 cell death.

To quantitatively compare the lysosomal change, we used total VAC to compare the lysosomal response between different cell lines. VAC can be analyzed by flow cytometry using LysoTracker or AO staining. The mean value of LysoTracker or AO staining reflects the average VAC per cell and can be used to compare lysosomal response. The basal level of VAC was approximately equal in all four lines (Fig. 5D). TNF treatment resulted in an increase in LysoTracker staining (Fig. 5D, top panel) and AO staining (Fig. 5D, lower panel) in L929 cells after exposure to TNF. The PMCA4-deficient cell lines

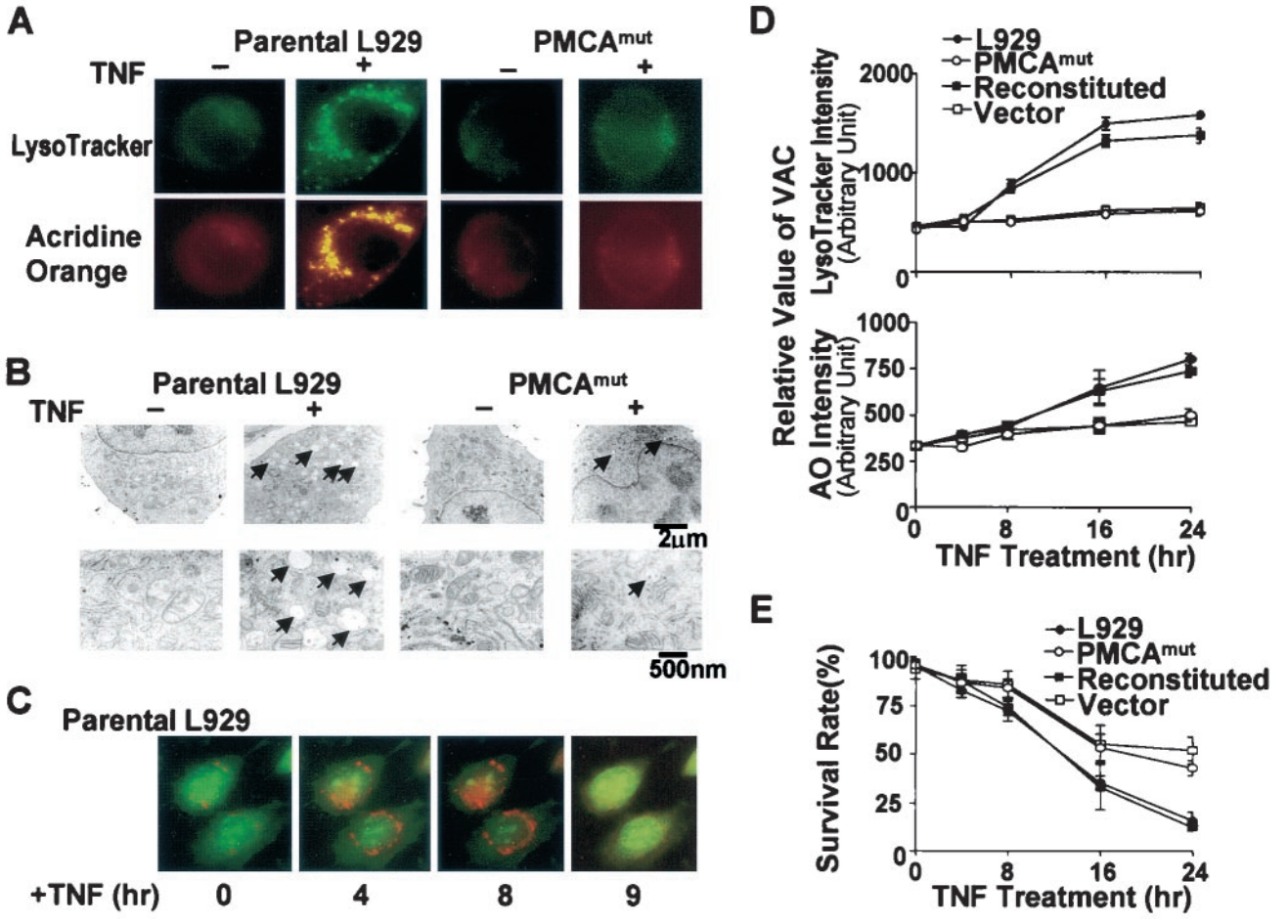

FIG. 5. TNF treatment increases VAC, and this effect is inhibited in PMCA4-deficient cells. The TNF-induced increase in VAC correlates with cell death. (A) Parental L929 and PMCA^{mut} cells were untreated (−) or treated with TNF (+) for 8 h. Cells were then stained with LysoTracker and AO and analyzed by fluorescence microscopy. (B) Electron microscopy was used to analyze ultrastructural features of parental and PMCA^{mut} cells after 8 h of TNF treatment. Arrows indicate enlarged lysosomes, which should be the major contributors to increased staining of acidic compartments in TNF-treated parental cells observed in panel A. Bars indicate the magnification scale. (C) Lysosome changes in parental L929 cells treated with TNF for different periods of time. The cells were stained with AO. (D) Cells were treated with TNF for various periods of time as indicated. The value of VAC was measured by flow cytometry using LysoTracker or AO staining as described in the text. LysoTracker and AO intensity in live cells was plotted to show the relative change in VAC. Parental and reconstituted cells had a significantly larger increase in VAC in response to TNF than PMCA^{mut} and vector control cells. (E) The survival rate of the cells shown in panel A is shown. The level of the increase in VAC (panel A) correlated with the rate of cell death (panel B).

(PCMA^{mut} and vector transfected) exhibited a much smaller average increase in VAC in response to TNF compared to the cells with normal levels of PMCA4 (the parental and reconstituted cell lines). These data support the hypothesis that the mutation in PMCA4 impaired the TNF-induced lysosomal response. The reduced lysosomal response (Fig. 5D) was correlated with an increased rate of cell survival in the PMCA4-deficient cell lines (Fig. 5E).

Calcium-enhanced lysosomal exocytosis is responsible, at least in part, for lack of TNF-induced increase in VAC in PMCA^{mut} cells. Calcium is known to stimulate lysosomal exocytosis in a number of different cell types, including fibroblasts (2, 68, 69). Therefore, it is possible that increased $[Ca^{2+}]_i$ in TNF-stimulated PMCA^{mut} cells promotes lysosome exocytosis. This could impede the increase in lysosomal mass observed in parental cells. To test this hypothesis, we measured lysosomal exocytosis in TNF-treated parental and PMCA^{mut} cells. Dextran can be imported into the cell by endocytosis and retained within lysosomes (21). Thus, pulse-chase experiments can be used to measure the rate of dextran exocytosis.

Lysosomes were loaded with dextran conjugated to tetramethylrhodamine, and the free dextran was then washed away. The cells were incubated for an additional 1 h to allow all conjugated dextran to be taken up into lysosomes (21). Cells were then treated with TNF for various times, between 0 and 24 h, and the retention of conjugated dextran was determined. As shown in Fig. 6A, conjugated dextran was released much more quickly in PMCA^{mut} cells than in parental cells. This is consistent with the hypothesis that PMCA^{mut} cells exhibit increased lysosomal exocytosis.

We also measured release of the lysosomal enzyme β-hexosaminidase in TNF-treated parental and PMCA^{mut} cells. As reported by others using different cells (69), a constitutive release of β-hexosaminidase was observed in L929 cells (Fig.

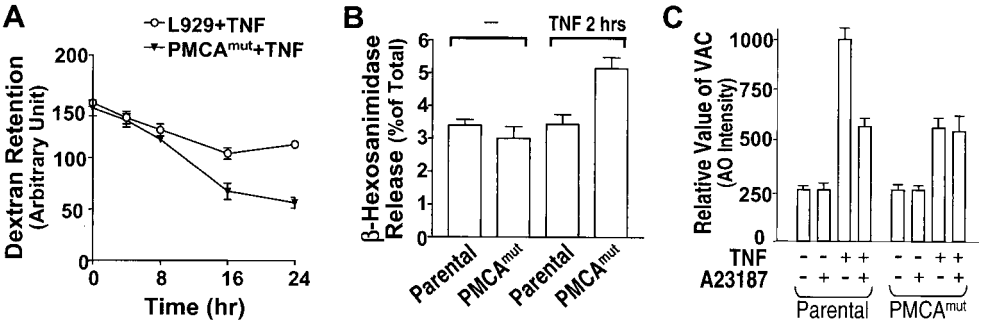

FIG. 6. Lysosomal exocytosis is more rapid in PMCA^{mut} cells than in parental cells. (A) Cells were incubated with tetramethylrhodamine-coupled dextran (2 mg/ml) for 1 h to load lysosomes with dextran. The cells were then washed and incubated in dextran-free medium for another hour and then treated with TNF. Dextran retention was measured by flow cytometry at the indicated time points after TNF treatment. (B) Parental and PMCA^{mut} cells were switched to fresh medium and untreated or treated with TNF for 2 h as indicated. Activity of the lysosomal enzyme β-hexosaminidase was measured in the medium and in the cells. The amount of enzyme in the medium is expressed as a percentage of the total enzyme level found in the cells. (C) Cells were treated with A23187 and TNF changes in VAC are shown.

6B). PMCA4 mutation did not influence the basal level of β-hexosaminidase release. Two hours of TNF treatment increased β-hexosaminidase release in PMCA^{mut} but not parental cells (Fig. 6B). The β-hexosaminidase release could not be measured at the later time of TNF treatment because of the spillover of intracellular components of dead cells. The data shown in Fig. 6A and 6B indicated that the lack of increase in VAC in TNF-treated PMCA^{mut} cells is due, at least in part, to increased exocytosis of lysosomes in these cells.

To assess whether the diminished lysosome response observed in PMCA^{mut} cells is mediated by elevated $[Ca^{2+}]_i$, we increased $[Ca^{2+}]_i$ by treating cells with either A23187 or $LaCl_3$. Treating parental L929 cells with A23187 inhibited the TNF-induced increase in VAC (Fig. 6C). PMCA^{mut} cells exhibited a much smaller increase in VAC in response to TNF, and this response was only slightly affected by A23187 (Fig. 6C). Similar results were obtained in the cells treated with $LaCl_3$ (data not shown). Thus, elevation of $[Ca^{2+}]_i$ clearly causes an inhibition of the lysosomal response.

Lysosomal response and cell death. To examine the requirement for the lysosomal response in TNF-induced cell death, we thought to test whether inhibition or enhancement of the increase in VAC influenced TNF-induced cell death. TNF-induced increase in VAC in parental L929 cells was inhibited by A23187 (Fig. 7A, left panel). The levels of the VAC were correlated with rate of cell death (Fig. 7A, right panel). PMCA^{mut} cells already had much less TNF-induced increase in VAC, and A23187 did not have much effect on VAC and cell death induced by TNF in PMCA^{mut} cells (Fig. 7A). These data support the idea that the inhibition of the lysosomal response diminished TNF-induced cell death.

We next wanted to compare the effect of inhibiting lysosomal exocytosis on TNF-induced cell death in PMCA^{mut} and parental cells. Unfortunately, at present no highly specific methods for inhibiting lysosomal exocytosis are available. Jasplakinolide, nocodazole, and MDL 12,330A are structurally unrelated compounds that are each known to inhibit lysosomal exocytosis (68), though these compounds also have many other effects on cells. jasplakinolide and nocodazole interfere with lysosomal exocytosis by stabilizing actin microfilaments and depolymerizing tubulin, respectively (68), whereas MDL inhibits lysosomal exocytosis via inhibition of adenylyl cyclase (68). We therefore tested the effect of these drugs on lysosomal exocytosis in L929 cells.

We confirmed that each of these drugs blocked A23187-induced release of β-hexosaminidase, which is a measure of lysosomal exocytosis, in L929 cells (data not shown). The three drugs did not affect L929 cell viability in 24 h, although jasplakinolide and nocodazole treatment caused a change in cell morphology. Thus, use of these drugs may provide useful information regarding the effect of the inhibition of lysosomal exocytosis on TNF-induced cell death. Cotreatment of parental L929 cells with TNF and these inhibitors did not significantly alter VAC (Fig. 7B, top left panel). In contrast, these inhibitors induced an increase in VAC in TNF-treated PMCA^{mut} cells (Fig. 7B, bottom left panel). These data suggest that lysosomal exocytosis in TNF-treated parental cells is low; hence, the effect of the inhibitors is barely seen. On the other hand, PMCA^{mut} cells have enhanced lysosomal exocytosis, and therefore the effect of each of these inhibitors is readily apparent. None of these drugs influenced TNF-induced cell death in parental cells (Fig. 7B, top right panel). In contrast, each of these drugs impaired cell survival in TNF-treated PMCA^{mut} cells, so that cell death occurred at a level similar to that seen in the parental line (Fig. 7B, bottom right panel). These findings further support the idea that lysosomes are involved in cell death.

It is known that indigestible solutes such as sucrose can cause lysosome fusion, which results in the formation of large lysosomes called sucrosomes (12, 35, 80). Culturing parental L929 and PMCA^{mut} cells in the presence of 0.03 M sucrose resulted in a significant increase in VAC; in contrast, 0.03 M glucose did not have such an effect (Fig. 7C, left panel). Both cell lines were healthy in either sucrose- or glucose-containing medium. In a second experiment, we cultured parental and PMCA^{mut} cells in either sucrose- or glucose-containing medium for 12 h to permit the formation of sucrosomes prior to TNF exposure. Incubation in sucrose significantly impaired the cell survival rate in TNF-treated PMCA^{mut} cells, whereas incubation in glucose had no effect on survival rate (Fig. 7C, right panel). The effect of sucrose on parental cells was much less pronounced (Fig. 7C, right panel). These data further suggest

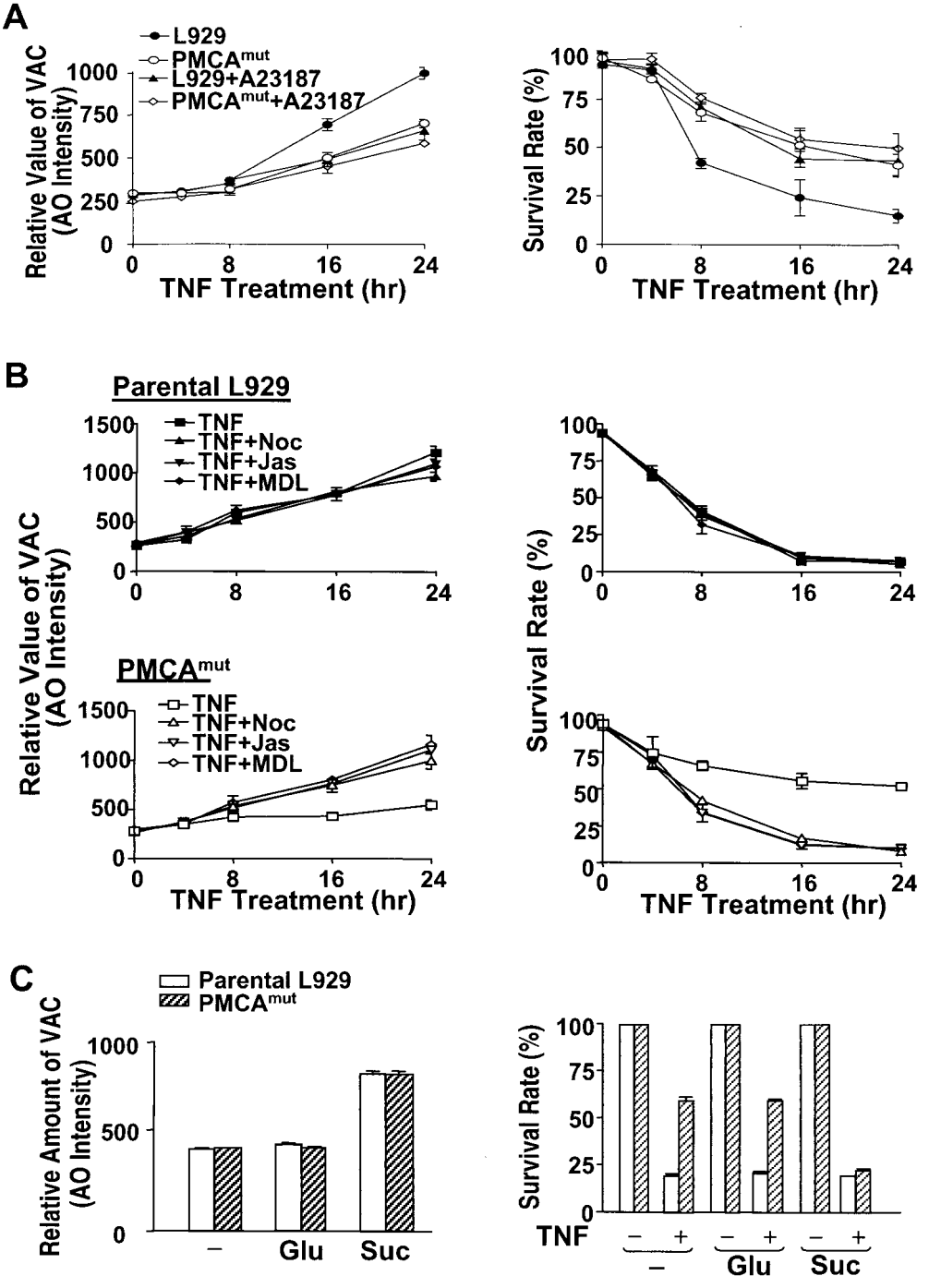

FIG. 7. Inhibition of TNF-induced increase in VAC in parental L929 cells increases survival rate, and enhancing VAC increases TNF-induced cell death in PMCA4^{mut} cells. (A) Cells as indicated were treated with TNF in the presence or absence of A23187 for different periods of time. VAC (left panel) and cell viability (right panel) were measured. A23187 inhibited TNF-induced increase in VAC and cell death in parental cells. (B) Parental L929 (top panels) and PMCA^{mut} (lower panels) cells were treated with TNF in the presence or absence of different inhibitors of exocytosis as indicated: nocodazole (Noc), 10 μM; jasplakinolide (Jas), 0.3 μM; and MDL-12330A (MDL), 50 μM. VAC (left panels) and cell viability (right panels) were measured at different time points after TNF treatment. The exocytosis inhibitors did not influence the TNF-induced increase in VAC and cell death in parental cells. In contrast, inhibition of exocytosis enhanced the TNF-induced increase in VAC and cell death in PMCA^{mut} cells. (C) Parental and PMCA^{mut} cells were treated with either 0.3 mM sucrose (Suc) or 0.3 mM glucose (Glu) as indicated. The formation of sucrosomes induced by 0.3 mM sucrose was detected by AO staining, as shown in the left panel. The survival rate of these cells in response to TNF treatment is shown in the right panel. Sucrosomes enhanced TNF-induced cell killing in PMCA^{mut} cells.

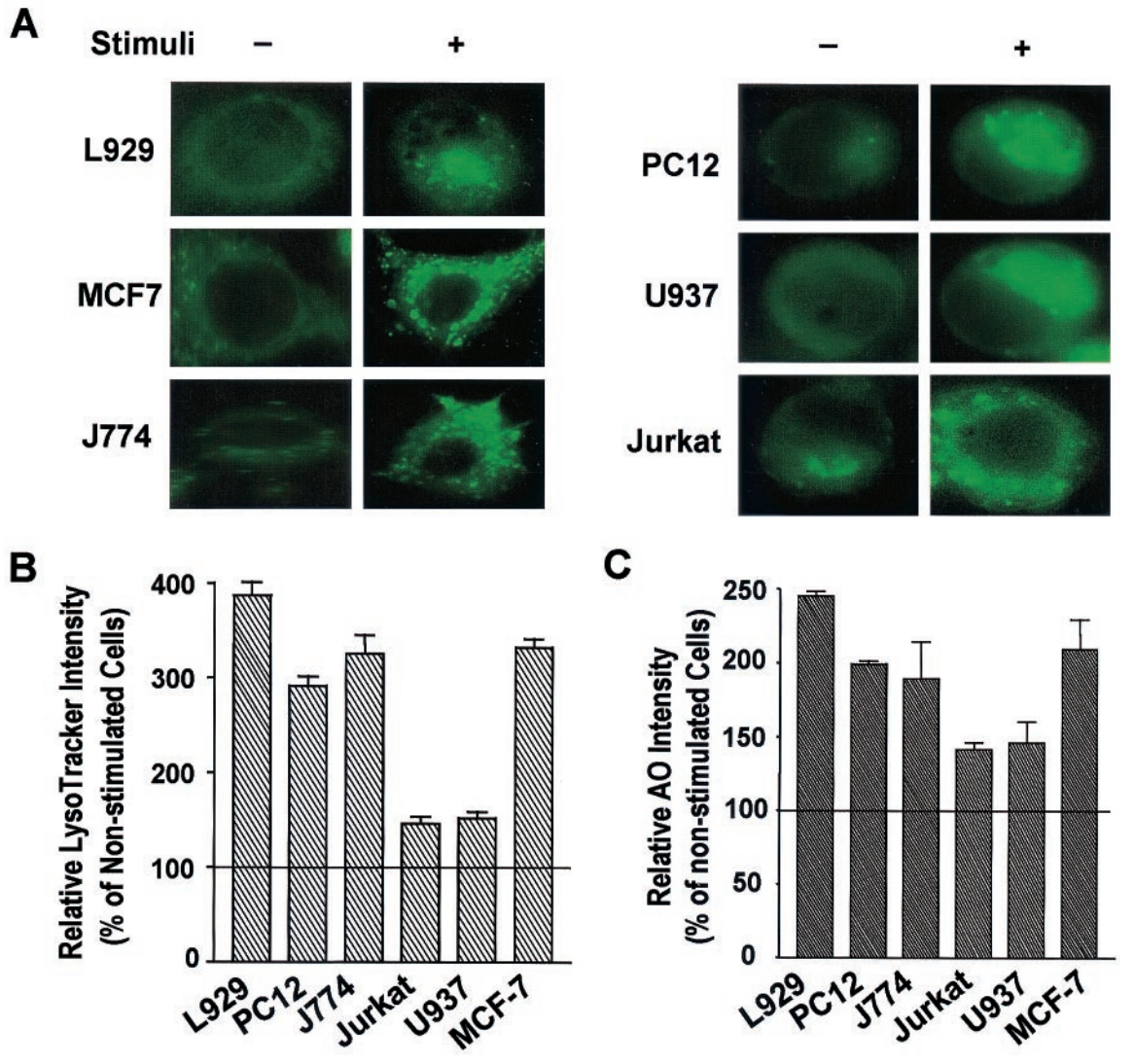

FIG. 8. Lysosomal response in different models of cell death. Several different cell culture systems were used to evaluate the change in VAC during the cell death process. L929 and MCF-7 cells were treated with TNF (100 ng/ml) for 8 h; PC12 cells were serum deprived for 6 days; J774 cells were treated with oxidized LDL (100 μg/ml) for 3 days; Jurkat cells were treated with Fas antibody (0.5 μg/ml) for 3 h; and U937 cells were treated with ceramide (100 μM) for 4 h. (A) Lysosomes were stained with LysoTracker and morphologically analyzed by fluorescence microscopy. (B and C) VAC was measured using LysoTracker staining (B) or AO staining (C). The relative LysoTracker or AO intensity is expressed as percent change from the control and was calculated by dividing the arbitrary fluorescence intensity unit number by that of corresponding untreated samples.

that the TNF resistance in PMCA^{mut} cells is related to lysosome function.

Cell death is generally associated with an increase in VAC. We next examined lysosomes in several different cell types that were exposed to various death stimuli. L929 and MCF-7 cells were treated with TNF; PC12 cells were serum deprived; J774 cells were treated with oxidized LDL; Jurkat cells were treated with a Fas antibody; and U937 cells were treated with ceramide. As shown in Fig. 8A, increased LysoTracker staining was observed in each of the samples exposed to a death stimulus. The relative VAC is shown in Fig. 8B and 8C. VAC changes varied among the different cell types. The increase in VAC did not correlate with the type of cell death (either apoptotic or necrotic), but rather seemed to be related to whether the cells were adherent or nonadherent. Suspended cells (Jurkat and U937 cells) exhibited much fewer lysosomal changes than adherent cells (L929, PC12, J774, and MCF-7 cells), which is probably due to suspended cells' having less cytosole than adherent cells. Nevertheless, an increase in VAC is a common event across many, if not all, cell death processes, including apoptosis and necrosis.

DISCUSSION

Using a random mutagenesis approach, we found that disruption of the PMCA4 gene produced a resistance to TNF-induced cell death in L929 cells (Fig. 1). We further demonstrated that a modest elevation in $[Ca^{2+}]_i$ underlies the resistance to TNF-induced cell death in PMCA^{mut} cells (Fig. 1 and 2). The calcium-mediated resistance to cell death ap-

peared to be related to lysosome function (Fig. 4). Increased lysosomal volume is a general characteristic of various cell death processes (Fig. 5 and 8). Calcium-promoted lysosomal exocytosis (Fig. 6 and 7) accounted, at least in part, for the inhibition of TNF-induced increase of lysosome volume observed in PMCA^{mut}, which in turn diminished TNF-induced cell death.

Elevation in $[Ca^{2+}]_i$ has long been known to induce apoptotic or necrotic cell death. Multiple mechanisms can mediate this prodeath effect of calcium, which has been studied intensively (59). However, while an antideath effect of calcium has been reported in a number of different cell systems (20, 52, 70), this effect of calcium has largely been neglected (59). Here we provide genetic evidence to support the hypothesis that calcium does indeed have antideath effects. The prodeath effects of calcium on cell death vary considerably in different cell types. The antideath effect of calcium may be similarly dependent on cell type, as calcium promotes lysosomal exocytosis in many, but not all, types of cells (2). It has been reported that Ca^{2+} concentrations between 1 and 5 μM are optimal for exocytosis of lysosomes in permeabilized cells (69). The exocytosis of lysosomal content was detected in our system (intact cells) when the intracellular Ca^{2+} concentration was ≈200 nM. It is possible that the local concentration of Ca^{2+} in certain cell compartments of our cell systems had reached the micromolar range or that 200 nM Ca^{2+} is sufficient to promote lysosomal exocytosis in live cells. Our data did not exclude the possibility that the inhibition of TNF-induced increase in VAC by calcium was also mediated at a level of lysosome biogenesis.

The transcription factor MEF2 was recently shown to be important in regulating neuronal survival during differentiation and depolarization (53, 63). p38 mitogen-activated protein kinase also plays a critical role in neuronal survival, since p38 activates MEF2. In contrast to its protective function in neurons, MEF2 promotes apoptosis in T cells. This process is thought to be mediated by enhancing the expression of Nur77 (92). L929 cells had very low levels of MEF2 activity, based on a gel shift assay (data not shown). We did not detect any differences in MEF2 activity between parental and PMCA^{mut} cells or between TNF-stimulated and nonstimulated cells (data not shown). p38 was activated by TNF treatment, but inhibition of p38 kinase activity did not alter TNF-induced cell death in either parental or PMCA^{mut} cells (data not shown). Thus, resistance to TNF-induced cell death in PMCA4-deficient cells is unlikely to be related to the p38-MEF2 pathway.

Activation of caspase 8 plays a key role in TNF-induced apoptosis in a number of different types of cells, including MCF-7 cells (74, 78). However, caspase 8 was not involved in TNF-induced death of L929 cells (86). Thus, the lysosomal response during cell death can occur in the absence of caspase 8 activation. In addition, the intracellular calcium concentration seems to have no effect on caspase 8 activation, since treatment of MCF-7 cells with A23187 did not influence TNF-induced caspase 8 activation (data not shown). There are reports suggesting the existence of both caspase-dependent and caspase-independent death pathways (6, 10, 16, 17, 30, 39, 40, 46, 55, 79). Expression of Bax in mammalian cells caused cell death with typical apoptotic phenotypes. Inhibition of caspases by zVAD prevented the cleavage of nuclear and cytosolic substrates of caspases and DNA fragmentation, but failed to prevent the reduction of mitochondrial membrane potential and production of ROS (90).

Interestingly, cell death in the presence of caspase inhibition was associated with cytoplasmic vacuolation (90), which is likely to be the same lysosomal enlargement observed in our experiments. Overexpression of mammalian Bax imposes a lethal phenotype in both *Saccharomyces cerevisiae* and *Schizosaccharomyces pombe* (26, 29, 38, 54). The mechanism by which Bax induces yeast cell death is believed to be similar to that in mammals (93). Yeast cells lack caspases, and their death does not show nuclear fragmentation, but rather massive vacuolization of the cytoplasm (93). This is similar to the morphology of human cells expressing Bax in the presence of a caspase inhibitor (90) and L929 cells that were stimulated with TNF. Thus, the signaling pathway that leads to lysosomal responses may be parallel to the caspase pathway. In support of this possibility, there are a number of reports showing that inhibition of caspases blocked nuclear events of apoptosis but not cell death or only delayed cell death (6, 10, 16, 17, 32, 39, 46, 55).

Mitochondria play an important role in many cell death processes (42). Treating L929 cells with TNF in the presence of the ROS scavenger butylated hydroxyanisole inhibited the increase in VAC (data not shown), suggesting that the lysosomal response is downstream of TNF-induced mitochondrial changes. Since there was no detectable cytochrome *c* released from the mitochondria of TNF-treated L929 cells (24), cytochrome *c* released from mitochondria may not be required for the lysosomal enlargement observed in our experiments. However, the involvement of other apoptogenic factors released from mitochondria cannot be excluded.

Since programmed cell death is an ordered process, it is likely that lysosomes were responsible for the self-digestion during the course of cell death. Previous studies have provided a large body of evidence suggesting that lysosomes are involved in cell death processes (7, 15, 36, 62, 65, 67, 91). In surveying the literature, we found a number of studies in which increases in the number and size of lysosomes were actually recorded in many electron photomicrographs of apoptotic or necrotic cells, but unfortunately, most of these results have been overlooked (18, 71, 72, 81). The lack of a thorough evaluation of the general involvement of lysosomes in the cell death program is probably related to the lack of a means to evaluate the overall lysosomal changes in cells. The PMCA^{mut} cell line provided an opportunity for us to evaluate the lysosomal changes that occur during the cell death process and to use VAC as an index for lysosomal change. Our data demonstrate that an increase in VAC is a common event in cell death that occurs in response to diverse stimuli.

Increase of lysosomal volume in processes such as TNF-induced cell death appears to be an execution event, as treatment with A23187 inhibits the increase and can effectively impede cell death after initiation of the apoptotic signal (data not shown). However, in certain cases, lysosomes may be also be involved in the initiation of cell death. Autophagy observed in nerve growth factor-deprived neurons (91) and in tamoxifen-treated MCF-7 cells (8) may represent an initial compensatory response to the absence of a growth signal (13). This may act as both a trigger and an executor of cell death. Translocation of a lysosomal protease, cathepsin B or D, to the cytosol was shown to promote mitochondrial release of cyto-

chrome *c* and apoptosis (28, 66). Accidental leakage of lysosomes in certain pathological situations or during aging may activate the apoptosis pathway or target other cellular organelles, such as mitochondria, to enhance the death signal (77). This possibility may underlie the observation that lysosome leakage occurs prior to mitochondrial and nuclear events in certain instances of cell death (28, 66).

Taken together, our data suggest a mechanism for the antideath effect of calcium and support the idea that lysosomes are not merely the final station of the endocytic pathway (2). In addition to their housekeeping role, lysosomes can indeed function as suicide bags, as Christian de Duve proposed in the late 1950s (14). Nuclear digestion (DNA fragmentation and nucleus condensation) has been well accepted as an essential event in programmed cell death. Lysosome-mediated cytosolic digestion may be as important as nuclear degradation in the cell death process. The increase in the volume of acidic compartments could be another hallmark of dying cells.

ACKNOWLEDGMENTS

We thank Ulf T. Brunk, Sandra L. Schmid, and Bruce Beutler for helpful comments and Janet V. Kuhns for excellent secretarial assistance.

This work was supported by U.S. Public Health Service grant no. AI41637 from the National Institute of Allergy and Infectious Diseases and California Cancer Research Program Subcontract no. 99-00521V-10121.

REFERENCES

1. **Aggarwal, B. B., R. A. Aiyer, D. Pennica, P. W. Gray, and D. V. Goeddel.** 1987. Human tumour necrosis factors: structure and receptor interactions. Ciba Found. Symp. **131:**39–51.
2. **Andrews, N. W.** 2000. Regulated secretion of conventional lysosomes. Trends Cell Biol. **10:**316–321.
3. **Beutler, B., and A. Cerami.** 1986. Cachectin and tumour necrosis factor as two sides of the same biological coin. Nature **320:**584–588.
4. **Beutler, B., and A. Cerami.** 1988. Tumor necrosis, cachexia, shock, and inflammation: a common mediator. Annu. Rev. Biochem. **57:**505–518.
5. **Beyaert, R., and W. Fiers.** 1994. Molecular mechanisms of tumor necrosis factor-induced cytotoxicity: what we do understand and what we do not. FEBS Lett. **340:**9–16.
6. **Bouchon, A., P. H. Krammer, and H. Walczak.** 2000. Critical role for mitochondria in B cell receptor-mediated apoptosis. Eur. J. Immunol. **30:**69–77.
7. **Brunk, U. T., and I. Svensson.** 1999. Oxidative stress, growth factor starvation and Fas activation may all cause apoptosis through lysosomal leak. Redox Rep. **4:**3–11.
8. **Bursch, W., A. Ellinger, H. Kienzl, L. Torok, S. Pandey, M. Sikorska, R. Walker, and R. S. Hermann.** 1996. Active cell death induced by the antiestrogens tamoxifen and ICI 164 384 in human mammary carcinoma cells (MCF-7) in culture: the role of autophagy. Carcinogenesis **17:**1595–1607.
9. **Carswell, E. A., L. J. Old, R. L. Kassel, S. Green, N. Fiore, and B. Williamson.** 1975. An endotoxin-induced serum factor that causes necrosis of tumors. Proc. Natl. Acad. Sci. USA **72:**3666–3670.
10. **Chi, S., C. Kitanaka, K. Noguchi, T. Mochizuki, Y. Nagashima, M. Shirouzu, H. Fujita, M. Yoshida, W. Chen, A. Asai, M. Himeno, S. Yokoyama, and Y. Kuchino.** 1999. Oncogenic Ras triggers cell suicide through the activation of a caspase-independent cell death program in human cancer cells. Onc. **18:** 2281–2290.
11. **Chow, S., and D. Hedley.** 1997. Flow cytometric measurement of intracellular pH, p. 9.3.1–9.3.10. *In* P. Robinson (ed.), Current protocols in cytometry. John Wiley & Sons, Inc., New York, N.Y.
12. **Cohn, Z. A., and B. A. Ehrenreich.** 1969. The uptake, storage, and intracellular hydrolysis of carbohydrates by macrophages. J. Exp. Med. **129:**201–225.
13. **Cuervo, A. M., and J. F. Dice.** 1998. Lysosomes, a meeting point of proteins, chaperones, and proteases. J. Mol. Med. **76:**6–12.
14. **de Duve, C.** 1959. Lysosomes, a new group of cytoplasmic particles in subcellular particles, p. 128–159. *In* T. Hayashi (ed.), Subcellular particles. The Ronald Press Co., New York, N.Y.
15. **Deiss, L. P., H. Galinka, H. Berissi, O. Cohen, and A. Kimchi.** 1996. Cathepsin D protease mediates programmed cell death induced by interferon-gamma, Fas/APO-1 and TNF-alpha. EMBO J. **15:**3861–3870.
16. **Doi, T., N. Motoyama, A. Tokunaga, and T. Watanabe.** 1999. Death signals from the B cell antigen receptor target mitochondria, activating necrotic and apoptotic death cascades in a murine B cell line, WEHI-231. Int. Immunol. **11:**933–941.
17. **Drenou, B., V. Blancheteau, D. H. Burgess, R. Fauchet, D. J. Charron, and N. A. Mooney.** 1999. A caspase-independent pathway of MHC class II antigen-mediated apoptosis of human B lymphocytes. J. Immunol. **163:**4115–4124.
18. **Fernandez-Segura, E., F. J. Canizares, M. A. Cubero, A. Warley, and A. Campos.** 1999. Changes in elemental content during apoptotic cell death studied by electron probe X-ray microanalysis. Exp. Cell Res. **253:**454–462.
19. **Fiers, W., R. Beyaert, W. Declercq, and P. Vandenabeele.** 1999. More than one way to die: apoptosis, necrosis and reactive oxygen damage. Oncology **18:**7719–7730.
20. **Franklin, J. L., and E. M. Johnson.** 1992. Suppression of programmed neuronal death by sustained elevation of cytoplasmic calcium. Trends Neurosci. **15:**501–508.
21. **Galloway, C. J., G. E. Dean, R. Fuchs, and I. Mellman.** 1988. Analysis of endosome and lysosome acidification in vitro. Methods Enzymol. **157:**601–611.
22. **Garcia, M. L., and E. E. Strehler.** 1999. Plasma membrane calcium ATPases as critical regulators of calcium homeostasis during neuronal cell function. Front. Biosci. **4:**D869–D882.
23. **Geisow, M. J.** 1984. Fluorescein conjugates as indicators of subcellular pH: a critical evaluation. Exp. Cell Res. **150:**29–35.
24. **Goossens, V., K. De Vos, D. Vercammen, M. Steemans, K. Vancompernolle, W. Fiers, P. Vandenabeele, and J. Grooten.** 1999. Redox regulation of TNF signaling. Biofactors **10:**145–156.
25. **Grondin, G., and A. R. Beaudoin.** 1996. Immunocytochemical and cytochemical demonstration of a novel selective lysosomal pathway (SLP) of secretion in the exocrine pancreas. J. Histochem. Cytochem. **44:**357–368.
26. **Gross, A., K. Pilcher, E. Blachly-Dyson, E. Basso, J. Jockel, M. C. Bassik, S. J. Korsmeyer, and M. Forte.** 2000. Biochemical and genetic analysis of the mitochondrial response of yeast to BAX and BCL-X(L). Mol. Cell. Biol. **20:**3125–3136.
27. **Guerini, D., E. Garcia-Martin, A. Zecca, F. Guidi, and E. Carafoli.** 1998. The calcium pump of the plasma membrane: membrane targeting, calcium binding sites, tissue-specific isoform expression. Acta Physiol. Scand. Suppl. **643:** 265–273.
28. **Guicciardi, M. E., J. Deussing, H. Miyoshi, S. F. Bronk, P. A. Svingen, C. Peters, S. H. Kaufmann, and G. J. Gores.** 2000. Cathepsin B contributes to TNF-alpha-mediated hepatocyte apoptosis by promoting mitochondrial release of cytochrome *c*. J. Clin. Investig. **106:**1127–1137.
29. **Harris, M. H., M. G. Vander Heiden, S. J. Kron, and C. B. Thompson.** 2000. Role of oxidative phosphorylation in Bax toxicity. Mol. Cell. Biol. **20:**3590–3596.
30. **Henkart, P. A.** 1996. ICE family proteases: mediators of all apoptotic cell death? Immunity **4:**195–201.
31. **Herscher, C. J., and A. F. Rega.** 1996. Presteady-state kinetic study of the mechanism of inhibition of the plasma membrane Ca^{2+}-ATPase by lanthanum. Biochemistry **35:**14917–14922.
32. **Hildeman, D. A., T. Mitchell, T. K. Teague, P. Henson, B. J. Day, J. Kappler, and P. C. Marrack.** 1999. Reactive oxygen species regulate activation-induced T cell apoptosis. Immunity **10:**735–744.
33. **Hsu, H., J. Xiong, and D. V. Goeddel.** 1995. The TNF receptor 1-asssociated protein TRADD signals cell death and NF-κB activation. Cell **81:**495–504.
34. **Isahara, K., Y. Ohsawa, S. Kanamori, M. Shibata, S. Waguri, N. Sato, T. Gotow, T. Watanabe, T. Momoi, K. Urase, E. Kominami, and Y. Uchiyama.** 1999. Regulation of a novel pathway for cell death by lysosomal aspartic and cysteine proteinases. Neuroscience **91:**233–249.
35. **Jahraus, A., B. Storrie, G. Griffiths, and M. Desjardins.** 1994. Evidence for retrograde traffic between terminal lysosomes and the prelysosomal/late endosome compartment. J. Cell Sci. **107:**145–157.
36. **Jia, L., R. R. Dourmashkin, P. D. Allen, A. B. Gray, A. C. Newland, and S. M. Kelsey.** 1997. Inhibition of autophagy abrogates tumour necrosis factor alpha induced apoptosis in human T-lymphoblastic leukaemic cells. Br. J. Haematol. **98:**673–685.
37. **June, C. H., R. Aby, and P. S. Rabinovitch.** 1997. Measurement of intracellular calcium ions by flow cytometry, p. 9.8.1–9.8.19. *In* P. Robinson (ed.), Current protocols in cytometry. John Wiley & Sons, Inc., New York, N.Y.
38. **Jurgensmeier, J. M., S. Krajewski, R. C. Armstrong, G. M. Wilson, T. Oltersdorf, L. C. Fritz, J. C. Reed, and S. Ottilie.** 1997. Bax- and Bak-induced cell death in the fission yeast *Schizosaccharomyces pombe*. Mol. Biol. Cell **8:**325–339.
39. **Kawahara, A., Y. Ohsawa, H. Matsumura, Y. Uchiyama, and S. Nagata.** 1998. Caspase-independent cell killing by Fas-associated protein with death domain. J. Cell Biol. **143:**1353–1360.
40. **Kim, S. O., K. Ono, and J. Han.** Apoptosis by pan-caspase inhibitors in lipopolysaccharide-activated macropgages. Am. J. Physiol Lung Cell Mol. Physiol., in press.
41. **Kravchenko, V. V., Z. Pan, J. Han, J.-M. Herbert, R. J. Ulevitch, and R. D. Ye.** 1995. Platelet-activating factor induces NF-κB activation through a G protein-coupled pathway. J. Biol. Chem. **270:**14928–14934.
42. **Kroemer, G., and J. C. Reed.** 2000. Mitochondrial control of cell death. Nat. Med. **6:**513–519.
43. **Kull, F. C., and J. M. Besterman.** 1990. Drug-induced alterations of tumor necrosis factor-mediated cytotoxicity: discrimination of early versus late

stage action. J. Cell Biochem. **42:**1–12.
44. **Kusuzaki, K., H. Murata, H. Takeshita, S. Hashiguchi, T. Nozaki, K. Emoto, T. Ashihara, and Y. Hirasawa.** 2000. Intracellular binding sites of acridine orange in living osteosarcoma cells. Anticancer Res. **20:**971–975.
45. **Lang, I. M., and R. R. Schleef.** 1996. Calcium-dependent stabilization of type I plasminogen activator inhibitor within platelet alpha-granules. J. Biol. Chem. **271:**2754–2761.
46. **Lavoie, J. N., M. Nguyen, R. C. Marcellus, P. E. Branton, and G. C. Shore.** 1998. E4orf4, a novel adenovirus death factor that induces p53-independent apoptosis by a pathway that is not inhibited by zVAD-fmk. J. Cell Biol. **140:**637–645.
47. **Li, H., S. K. Kolluri, J. Gu, M. I. Dawson, X. Cao, P. D. Hobbs, B. Lin, G. Chen, J. Lu, F. Lin, Z. Xie, J. A. Fontana, J. C. Reed, and X. Zhang.** 2000. Cytochrome c release and apoptosis induced by mitochondrial targeting of nuclear orphan receptor TR3. Science **289:**1159–1164.
48. **Li, P., D. Nijhawan, I. Budihardjo, S. M. Srinivasula, M. Ahmad, E. S. Alnemri, and X. Wang.** 1997. Cytochrome c and dATP-dependent formation of Apaf-1/caspase-9 complex initiates an apoptotic protease cascade. Cell **91:**479–489.
49. **Liddil, J. D., R. T. Dorr, and P. Scuderi.** 1989. Association of lysosomal activity with sensitivity and resistance to tumor necrosis factor in murine L929 cells. Cancer Res. **49:**2722–2728.
50. **Lloyd, J. B.** 1996. The taxonomy of lysosomes and related structures. Subcell. Biochem. **27:**1–13.
51. **Lockshin, R. A., and J. Beaulaton.** 1981. Cell death: questions for histochemists concerning the causes of the various cytological changes. Histochem. J. **13:**659–666.
52. **Lotem, J., R. Kama, and L. Sachs.** 1999. Suppression or induction of apoptosis by opposing pathways downstream from calcium-activated calcineurin. Proc. Natl. Acad. Sci. USA **96:**12016–12020.
53. **Mao, Z., A. Bonni, F. Xia, M. Nadal-Vicens, and M. E. Greenberg.** 1999. Neuronal activity-dependent cell survival mediated by transcription factor MEF2. Science **286:**785–790.
54. **Marzo, I., C. Brenner, N. Zamzami, J. M. Jurgensmeier, S. A. Susin, H. L. Vieira, M. C. Prevost, Z. Xie, S. Matsuyama, J. C. Reed, and G. Kroemer.** 1998. Bax and adenine nucleotide translocator cooperate in the mitochondrial control of apoptosis. Science **281:**2027–2031.
55. **Mateo, V., L. Lagneaux, D. Bron, G. Biron, M. Armant, G. Delespesse, and M. Sarfati.** 1999. CD47 ligation induces caspase-independent cell death in chronic lymphocytic leukemia. Nat. Med. **5:**1277–1284.
56. **Miller, A. D., and C. Buttimore.** 1986. Redesign of retrovirus packaging cell lines to avoid recombination leading to helper virus production. Mol. Cell. Biol. **6:**2895–2902.
57. **Mohler, J. L., and Y. Sharief.** 1993. Flow cytometric assay of pinocytosis: correlation with membrane ruffling and metastatic potential in the Dunning R-3327 rat prostatic adenocarcinoma model. Cytometry **14:**826–831.
58. **Monney, L., R. Olivier, I. Otter, B. Jansen, G. G. Poirier, and C. Borner.** 1998. Role of an acidic compartment in tumor-necrosis-factor-alpha-induced production of ceramide, activation of caspase-3 and apoptosis. Eur. J. Biochem. **251:**295–303.
59. **Nicotera, P., and S. Orrenius.** 1998. The role of calcium in apoptosis. Cell Calcium **23:**173–180.
60. **Nixon, R. A., and A. M. Cataldo.** 1993. The lysosomal system in neuronal cell death: a review. Ann. N. Y. Acad. Sci. **679:**87–109.
61. **Novak, E. J., and P. S. Rabinovitch.** 1994. Improved sensitivity in flow cytometric intracellular ionized calcium measurement using fluo-3/Fura Red fluorescence ratios. Cytometry **17:**135–141.
62. **Ohsawa, Y., K. Isahara, S. Kanamori, M. Shibata, S. Kametaka, T. Gotow, T. Watanabe, E. Kominami, and Y. Uchiyama.** 1998. An ultrastructural and immunohistochemical study of PC12 cells during apoptosis induced by serum deprivation with special reference to autophagy and lysosomal cathepsins. Arch. Histol. Cytol. **61:**395–403.
63. **Okamoto, S., D. Krainc, K. Sherman, and S. A. Lipton.** 2000. Antiapoptotic role of the p38 mitogen-activated protein kinase-myocyte enhancer factor 2 transcription factor pathway during neuronal differentiation. Proc. Natl. Acad. Sci. USA **97:**7561–7566.
64. **Old, L. J.** 1985. Tumor necrosis factor (TNF). Science **230:**630–632.
65. **Ollinger, K., and U. T. Brunk.** 1995. Cellular injury induced by oxidative stress is mediated through lysosomal damage. Free Radic. Biol. Med. **19:** 565–574.
66. **Roberg, K., U. Johansson, and K. Ollinger.** 1999. Lysosomal release of cathepsin D precedes relocation of cytochrome c and loss of mitochondrial transmembrane potential during apoptosis induced by oxidative stress. Free Radic. Biol. Med. **27:**1228–1237.
67. **Roberg, K., and K. Ollinger.** 1998. Oxidative stress causes relocation of the lysosomal enzyme cathepsin D with ensuing apoptosis in neonatal rat cardiomyocytes. Am. J. Pathol. **152:**1151–1156.
68. **Rodriguez, A., I. Martinez, A. Chung, C. H. Berlot, and N. W. Andrews.** 1999. cAMP regulates Ca^{2+}-dependent exocytosis of lysosomes and lysosome-mediated cell invasion by trypanosomes. J. Biol. Chem. **274:**16754–16759.
69. **Rodriguez, A., P. Webster, J. Ortego, and N. W. Andrews.** 1997. Lysosomes behave as Ca^{2+}-regulated exocytic vesicles in fibroblasts and epithelial cells. J. Cell Biol. **137:**93–104.
70. **Rodriguez-Tarduchy, G., M. Collins, and A. Lopez-Rivas.** 1990. Regulation of apoptosis in interleukin-3-dependent hemopoietic cells by interleukin-3 and calcium ionophores. EMBO J. **9:**2997–3002.
71. **Schulze-Osthoff, K., A. C. Bakker, B. Vanhaesebroeck, R. Beyaert, W. A. Jacob, and W. Fiers.** 1992. Cytotoxic activity of tumor necrosis factor is mediated by early damage of mitochondrial functions: evidence for the involvement of mitochondrial radical generation. J. Biol. Chem. **267:**5317–5323.
72. **Sesso, A., D. T. Fujiwara, M. Jaeger, R. Jaeger, T. C. Li, M. M. Monteiro, H. Correa, M. A. Ferreira, R. I. Schumacher, J. Belisario, B. Kachar, and E. J. Chen.** 1999. Structural elements common to mitosis and apoptosis. Tissue Cell **31:**357–371.
73. **Shibata, M., S. Kanamori, K. Isahara, Y. Ohsawa, A. Konishi, S. Kametaka, T. Watanabe, S. Ebisu, K. Ishido, E. Kominami, and Y. Uchiyama.** 1998. Participation of cathepsins B and D in apoptosis of PC12 cells following serum deprivation. Biochem. Biophys. Res. Commun. **251:**199–203.
74. **Srinivasan, A., F. Li, A. Wong, L. Kodandapani, R. J. Smidt, J. F. Krebs, L. C. Fritz, J. C. Wu, and K. J. Tomaselli.** 1998. Bcl-xL functions downstream of caspase-8 to inhibit Fas- and tumor necrosis factor receptor 1-induced apoptosis of MCF7 breast carcinoma cells. J. Biol. Chem. **273:**4523–4529.
75. **Stinchcombe, J. C., and G. M. Griffiths.** 1999. Regulated secretion from hemopoietic cells. J. Cell Biol. **147:**1–6.
76. **Stinchcombe, J. C., L. J. Page, and G. M. Griffiths.** 2000. Secretory lysosome biogenesis in cytotoxic T lymphocytes from normal and Chediak Higashi syndrome patients. Traffic **1:**435–444.
77. **Stoka, V., B. Turk, S. L. Schendel, T. H. Kim, T. Cirman, S. J. Snipas, L. M. Ellerby, D. Bredesen, H. Freeze, M. Abrahamson, D. Bromme, S. Krajewski, J. C. Reed, X. M. Yin, V. Turk, and G. S. Salvesen.** 2001. Lysosomal protease pathways to apoptosis: cleavage of bid, not Pro-caspases, is the most likely route. J. Biol. Chem. **276:**3149–3157.
78. **Strasser, A., L. O'Connor, and V. M. Dixit.** 2000. Apoptosis signaling. Annu. Rev. Biochem. **69:**217–245.
79. **Susin, S. A., H. K. Lorenzo, N. Zamzami, I. Marzo, B. E. Snow, G. M. Brothers, J. Mangion, E. Jacotot, P. Costantini, M. Loeffler, N. Larochette, D. R. Goodlett, R. Aebersold, D. P. Siderovski, J. M. Penninger, and G. Kroemer.** 1999. Molecular characterization of mitochondrial apoptosis-inducing factor. Nature **397:**441–446.
80. **Swanson, J., B. Yirinec, E. Burke, A. Bushnell, and S. C. Silverstein.** 1986. Effect of alterations in the size of the vacuolar compartment on pinocytosis in J774.2 macrophages. J. Cell Physiol. **128:**195–201.
81. **Takemura, G., M. Ohno, Y. Hayakawa, J. Misao, M. Kanoh, A. Ohno, Y. Uno, S. Minatoguchi, T. Fujiwara, and H. Fujiwara.** 1998. Role of apoptosis in the disappearance of infiltrated and proliferated interstitial cells after myocardial infarction. Circ. Res. **82:**1130–1138.
82. **Tartaglia, L. A., T. M. Ayres, G. H. Wong, and D. V. Goeddel.** 1993. A novel domain within the 55 kd TNF receptor signals cell death. Cell **74:**845–853.
83. **Tewari, M., and V. M. Dixit.** 1995. Fas- and tumor necrosis factor-induced apoptosis in inhibited by the poxvirus *crmA* gene product. J. Biol. Chem. **270:**3255–3260.
84. **Tewari, M., and V. M. Dixit.** 1996. Recent advances in tumor necrosis factor and CD40 signaling. Curr. Opin. Genet. Dev. **6:**39–44.
85. **Tulsiani, D. R., A. Abou-Haila, C. R. Loeser, and B. M. Pereira.** 1998. The biological and functional significance of the sperm acrosome and acrosomal enzymes in mammalian fertilization. Exp. Cell Res. **240:**151–164.
86. **Vercammen, D., R. Beyaert, G. Denecker, V. Goossens, G. Van Loo, W. Declercq, J. Grooten, W. Fiers, and P. Vandenabeele.** 1998. Inhibition of caspases increases the sensitivity of L929 cells to necrosis mediated by tumor necrosis factor. J. Exp. Med. **187:**1477–1485.
87. **Wang, E., J. Michl, L. M. Pfeffer, S. C. Silverstein, and I. Tamm.** 1984. Interferon suppresses pinocytosis but stimulates phagocytosis in mouse peritoneal macrophages: related changes in cytoskeletal organization. J. Cell Biol. **98:**1328–1341.
88. **Wang, H. G., N. Pathan, I. M. Ethell, S. Krajewski, Y. Yamaguchi, F. Shibasaki, F. McKeon, T. Bobo, T. F. Franke, and J. C. Reed.** 1999. Ca2+-induced apoptosis through calcineurin dephosphorylation of BAD. Science **284:**339–343.
89. **Wang, X., K. Ono, S. O. Kim, V. Kravchenko, S. C. Lin, and J. Han.** 2001. Metaxin is required for tumor necrosis factor-induced cell death. EMBO Rep. **2:**628–633.
90. **Xiang, J., D. T. Chao, and S. J. Korsmeyer.** 1996. BAX-induced cell death may not require interleukin 1 beta-converting enzyme-like proteases. Proc. Natl. Acad. Sci. USA **93:**14559–14563.
91. **Xue, L., G. C. Fletcher, and A. M. Tolkovsky.** 1999. Autophagy is activated by apoptotic signalling in sympathetic neurons: an alternative mechanism of death execution. Mol. Cell. Neurosci. **14:**180–198.
92. **Youn, H. D., L. Sun, R. Prywes, and J. O. Liu.** 1999. Apoptosis of T cells mediated by Ca^{2+}-induced release of the transcription factor MEF2. Science **286:**790–793.
93. **Zha, H., H. A. Fisk, M. P. Yaffe, N. Mahajan, B. Herman, and J. C. Reed.** 1996. Structure-function comparisons of the proapoptotic protein Bax in yeast and mammalian cells. Mol. Cell. Biol. **16:**6494–6508.